A New High Data Rate M-OAM Modulation for IR-UWB Communication

K. HAMIDOUN, Z. OUABOU, R. ELASSALI, Y. ELHILLALI, A. REVINQ, K. ELBAAMRANI

***Abstract*—In this paper a new high data rate IR-UWB communication system is proposed. Our approach concerns two areas of applications: Multimedia communication systems and Intelligent Transportation system (ITS). This paper presents an original modulation schemes, called M-OAM (Orthogonal Amplitude Modulation) aiming to improve data rate. The main advantage of this modulation technique is its low complexity with a very high data rate. The performance of the proposed system is evaluated for different modulation schemes (MOAM) in AWGN and UWB channels. However, the system performance degraded due to the multipath effect. Thus, the contribution of S-RAKE receiver architecture in performance improvement is investigated. An other originality of this paper concerns the experimental tests performed on real conditions.**

***Index Terms*—UWB, orthogonal waveforms, M-OAM, PPM Pulse Position Modulation, Antipodal modulation, AWGN channel, S-RAKE.**

I. Introduction

ULTRA Wide Band technology is based on the transmission of very short pulses occupying a broadband. The first definition of UWB is given by Taylor [1]: all system whose fractional band B_{frac} is greater than or equal to 20% is an UWB system. The width of this band is given by the following equation:

$$B_{frac} = \frac{f_h - f_l}{f_c} \tag{1}$$

Where f_h and f_l represent the highest and the lowest -10 dB frequency points respectively. f_c is the central frequency.

The second definition of UWB is all system occupying a frequency band above $500MHz$. This definition has been adopted by the majority of involved parties.

Several properties favor the use of UWB technique such as: low probability of interception and detection, system simplicity, low cost, reduced average power consumption, low sensitivity to the near-far problem or immunity to interferences [2]. This physical layer radio technology offers many advantages, which make it a promising option for short range communication applications in severe environments in terms of propagation.

The improvement of data rate for many applications becomes a major interest for industry as well as researchers.

K. HAMIDOUN is with UPHF University, France/ CADI AYYAD University, Morocco (e-mail:k.hamidoun@gmail.com).

Z. OUABOU is with TIM Laboratory, National School of Applied Sciences, CADI AYYAD University, Morocco (e-mail: zaina.ouabou@gmail.com).

R. ELASSALI is with TIM Laboratory, National School of Applied Sciences, Morocco (e-mail: r.elassali@uca.ma).

Y. ELHILLALI is with the IEMN-DOAE Laboratory, UPHF University, Valenciennes, France (e-mail: yassin.elhillali@univ-valenciennes.fr).

A. RIVENQ is with the IEMN-DOAE Laboratory, UPHF University, France (e-mail: atika.menhaj@univ-valenciennes.fr).

K. ELBAAMRANI is with the National School of Applied Sciences (ENSA), Marrakesh, Morocco.

In the case of the wireless local area network (WLAN), the two new standards currently under development IEEE.802.11ac and IEEE.802.11ad can achieve a theoretical maximum throughput up to $8Gbit/s$ in the $5GHz$ band and $7Gbit/s$ in $60GHz$ frequency band respectively [3],[4]. Indeed, the objective of this paper is to propose a new adaptive system which can reach a very high data rate, meeting the requirements of service quality for short range communications in intelligent transportation systems.

IR-UWB technology is generally based on very short duration waveforms on the order of nanoseconds. Different pulse shapes may be combined with UWB, and the most used are Gaussian and its derivatives pulses, or Manchester pulses based on orthogonal polynomials [5]. It has been shown that the most suitable waveforms to UWB communication systems are the second Gaussian derivative and orthogonal polynomials including Gegenbauer and Hermite polynomials [8]. Thus, the modified Gegenbauer functions (MGF) will be used in our new modulation.

This paper is organized as follows. Section II describes the orthogonal polynomials used in IR-UWB systems. In this section, we focus on the properties of two waveform families: modified Hermite and modified Gegenbauer functions. Subsequently, the third section presents the proposed system based on M-OAM modulations. Simulation and theoretical results are illustrated under AWGN channel conditions in section IV and V. Then, result study of the UWB channel IEEE.802.15.3a is given with reception solutions. Finally, our system is validated by experimental tests performed in our laboratory under real conditions.

II. IR-UWB COMMUNICATION SYSTEM

A. Orthogonal polynomials

It has been proved in [7], [8], that Gegenbauer and Hermite pulses give the best results for UWB communications compared to the other orthogonal waveforms. In this section, a short presentation of these two waveforms is given.

1) Modified Hermite functions: Hermite functions are defined by the following equation:

$$h_n(t) = (-1)^n e^{\frac{t^2}{4}} \frac{d^n}{dt^n} e^{\frac{-t^2}{2}} \tag{2}$$

Where $n = 0, 1, 2...$ *and* $t \in]-\infty, +\infty[$.

2) Modified Gegenbauer functions: These waveforms have been developed in IEMN DOAE laboratory for communication applications [7]-[9].

Gegenbauer polynomials are defined on the interval $[-1, 1]$ and satisfies the differential equation of second order defined as follows:

$$G_{(n,\beta)}(x) = 2(1 + (n + \beta - 1)/n)xG_{(n-1,\beta)}(x) - (1 + (n + 2\beta - 2)/n)G_{(n-2,\beta)}(x) \tag{3}$$

It should be noted that other previous works are interested in the comparison of these two waveform families ([7], [8]). In [7], the authors focus on the improvement of Hermite functions defined first in [2]. Subsequently, the thesis [8] comes to continue in the same direction. As a conclusion, they found that Gegenbauer waveforms give better performance than Hermite waveforms. In our case, we use the Gegenbauer polynomials as orthogonal waveforms to provide a high data rate modulation.

B. Classical IR-UWB Modulations

To modulate the pulse train and thus encode information to be transmitted, three main solutions are presented in the literature:

1) Pulse Position Modulation (PPM):: This technique consists in shifting the pulse position in time according to the symbol to be transmitted [15], [19]. For example $+\delta$ to send 0 and -δ to send 1. The expression of modulated signal is given by equation 4:

$$s(t) = \sum_{j=1}^{+\infty} m(t - jT - \delta d_j) \tag{4}$$

d_j : Transmitted bit 0,1
δ : Shift parameter
T : Repetition period
m(t) : Used waveform

2) Antipodal modulation:: Antipodal modulation consists in encoding information by transmitting the pulse with a phase shift of 0 or 1 [15], [16]. The expression of the modulated signal is given by the following equation:

$$s(t) = \sum_{k=-\infty}^{+\infty} a_k m(t - kT_s) \tag{5}$$

With:
T_s : the pulse repetition period
m(t) : the used waveform
$a_k \in$ {-1,1}

3) Pulse Amplitude Modulation (PAM): PAM modulation is an alternative to pulse position modulation. This technique involves varying the amplitude of the transmitted pulses to encode different states. The shape of the transmitted signal is given by the following expression:

$$s(t) = \sum_{j=1}^{+\infty} d_j m(t - jT) \tag{6}$$

Where: d_j : a binary code; T : the repetition period; $m(t)$: the used waveform.

III. PROPOSED UWB HIGH DATA RATE MODULATIONS

In this section, a new approach of IR-UWB modulation will be presented. The BER performances in terms of SNR for this new system will be evaluated by simulations, analytical studies and real tests. This study has been established in the perfect synchronization case between the transmitter and the receiver. The receiver and the transmitter block diagrams for UWB communication system are described in Figure 1. The coder and decoder blocks are modified in order to reach a high data rate.

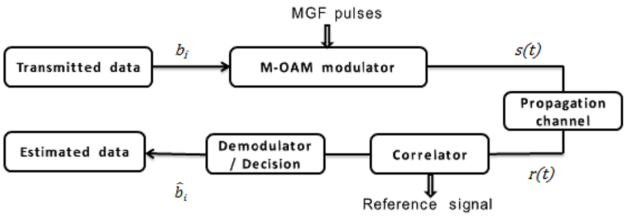

Fig. 1: Proposed system

A. PPM-Bipolar

The proposed PPM-bipolar modulation is based on the association of PPM and antipodal modulations. Each symbol is characterized by 2 bits, the first bit sent determines the sign of the pulse and the second determines its position. The symbol equation is:

$$x_i(t) = (2S_{iMSB} - 1)m(t + (2S_{iLSB} - 1)T) \tag{7}$$

With

$$m(t) = 2\alpha K t exp(-\alpha t^2) \tag{8}$$

S_i: sent symbol
m(t): used waveform
T : time interval
LSB: Low Significant Bit
MSB: Most Significant Bit

Figure 2 shows a series of modulated monocycle pulses with the PPM-Bipolar.

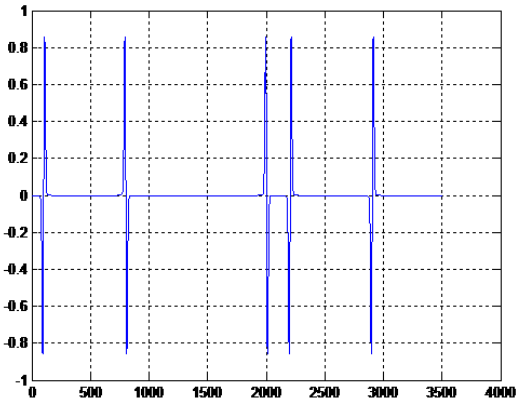

Fig. 2: PPM-bipolar modulation

Our proposed system is inspired from the PPM-Bipolar modulation, detailed previously. In the case of M-OAM modulations, the orthogonality properties related to the Gegenbauer functions are used in order to increase data rate. As we will see in the next section, our system provides high robustness with a low complexity and a simple implementation.

B. M-OAM Modulations

The idea of M-OAM modulations consists of replacing the carriers used on QAM modulation with orthogonal waveforms. Therefore, the $cosin$ of QAM modulation is replaced by an order of Gegenbauer polynomials and sin by a second order. This modulation provides a very high data rate and it's robust against the propagation channel effects [16]-[18].

The principle of modulations M-OAM is to modulate the transmitted pulse in M states. M is a multiple of 2, M = 2n when n is the number of bit per symbol. Increasing n increases the number of bits transmitted per symbol and hence the data rate offered. Depending on the value of n, we present three cases of modulations: 4-OAM, 16-OAM and 64-OAM and the particular cases 8-OAM and 32-OAM with odd values of n.

Table I gives a comparison of data rate between our system and the conventional UWB system.

TABLE I: Data rate of each M-OAM modulation, where D is the data rate of conventional UWB system

n	M states	Modulation	Data rate
2	4	4-OAM	2D
3	8	8-OAM	3D
4	16	16-OAM	4D
5	32	32-OAM	5D
6	64	64-OAM	6D

1) 4-OAM Modulation: This modulation is based on the same principle of bipolar-PPM modulation, but here we use Gegenbauer functions. Subsequently, this modulation allows doubling the data rate value compared to the classical UWB system. However, the system sensitivity to noise and the receiver complexity remains to be checked.

Table II presents the four obtained symbols:

TABLE II: Symbols of 4-OAM modulation

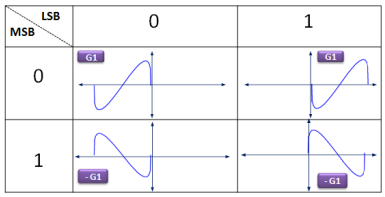

Using our new technique, the signal is quantified on multi-bit and the correlation is optimized thereby increasing the performance of the correlator.

To find the bits sent, the peak position and its polarity are evaluated. Therefore, the first step is the correlation between the received signal and the reference (Pulse used in transmitter block). Subsequently, the polarity and the position of peak correlation give the MSB and LSB values respectively.

The algorithm in figure 3 corresponds to the decoding algorithm applied to signals modulated with 4-OAM technique.

2) 16-OAM Modulation: This modulation involves sending $4bits/symbol$. Therefore, the data rate of our system will be improved. To obtain 16-OAM symbol, the first waveform G1 coding the first two bits in 4-OAM modulation is added to the second waveform G2 coding the two following bits.

Table III shows the symbols obtained by 16-OAM modulation.

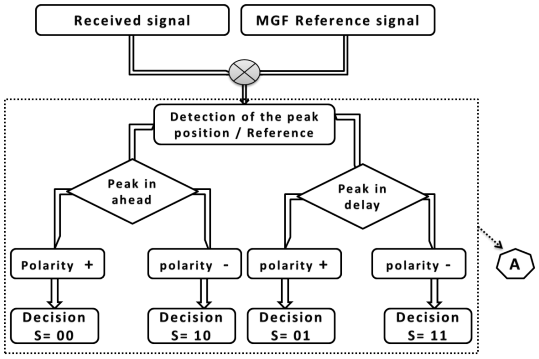

Fig. 3: Decoding algorithm of 4-OAM

TABLE III: Symbols of 16-OAM modulation

This modulation increases the data rate. But the difficulty is to analyse the signal at reception and to be able to decode it. It is necessary to find a good compromise between high speed and system complexity.

The equation of received signal after channel propagation is:

$$R(t) = s(t) * h(t) + n(t) \tag{9}$$

The signal obtained after correlation with the reference signal is given by the equation (10) :

$$r(t) = R(t) * m_i(t) + n(t) * m_i(t) \tag{10}$$

$m_i(t)$ is the used waveform (G1 or G2).

The algorithm described in figure 4 corresponds to steps of decoding signals modulated in 16-OAM. The block A is described by figure 3.

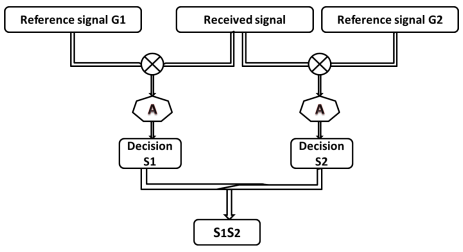

Fig. 4: Decoding algorithm of 16-OAM

3) 64-OAM modulation: In this case, the signal is composed of three sub-symbols; each one is a combination of a position and a phase represented by an order of Gegenbauer polynomials and different of the following sub-symbol. Three levels are used in this case (G1, G2 and G3). The transmitted signal is the sum of three sub-symbols. Consequently, modulation 64-OAM multiplies the data rate by a factor of six compared to a classical UWB system.

TABLE IV: Symbols of 64-OAM modulation

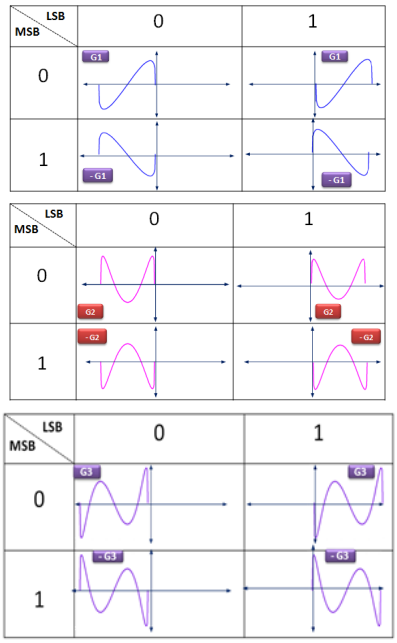

4) 8-OAM modulation: 8-OAM modulation sends $3bits/symbol$. In fact, the first two bits are encoded in 4-OAM modulation with $G1$ waveform, and the third bit is modulated in PPM with the second order $G2$. As a result, 8-OAM modulation increases the data rate by a factor of three compared to the conventional UWB system.

Table V gives the possible combinations of 8-OAM modulation.

TABLE V: Symbols of 8-OAM modulation

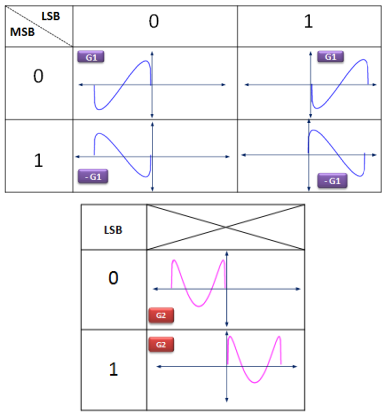

5) 32-OAM modulation: This modulation is also a particular case like 8-OAM, because the value of N is odd. Indeed, the 32-OAM sends $5bits/symbol$. So, the first four bits are modulated in the same way as the 16-OAM modulation with orthogonal waveforms G1 and G2, while the fifth bit is modulated in PPM with G3. Thus, the 32-OAM modulation increases the speed by five compared to a conventional ULB system.

Table VI illustrates the possible combinations of 32-OAM modulation.

TABLE VI: Symbols of 32-OAM modulation

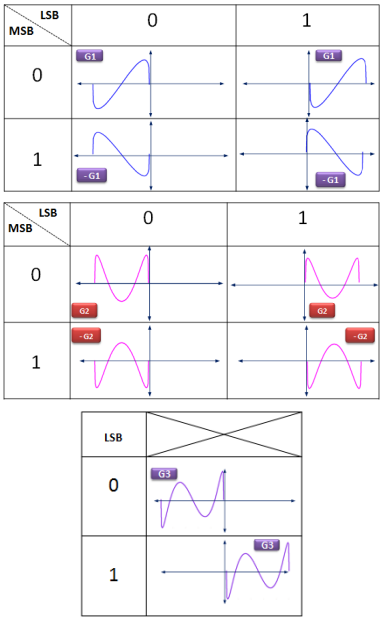

IV. PERFORMANCE OF PROPOSED SYSTEM ON A PERFECT AWGN CHANNEL

Performances of the proposed system are evaluated by simulation using AWGN channel and the computation of BER versus signal to noise ratio SNR.

Figure 5 presents a comparison between different orthogonal waveforms, and the classical UWB waveforms. We notice that 4-OAM modulation gives same performances for different pulses. This proves the robustness of our system.

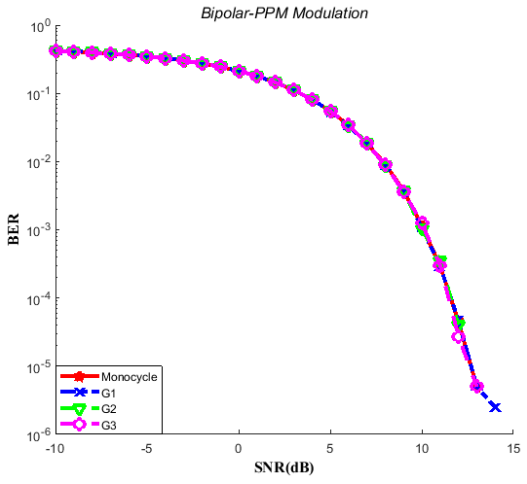

Fig. 5: Performance of Bipolar-PPM modulation for different waveforms

To evaluate the performance and robustness of M-OAM modulations, the BER values is calculated for M = 4; 16; 64 under AWGN channel conditions (figure 6).

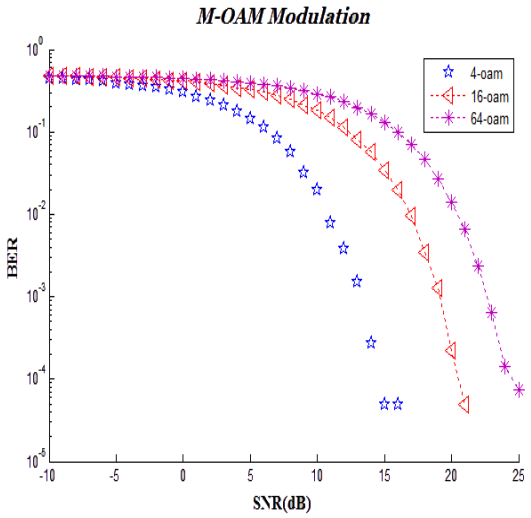

Fig. 6: M-OAM Modulation

We note that the BER decreases exponentially when the SNR increases. In addition, for low M value, the modulation is more robust to noise. By using 4-OAM modulation, we can establish a good communication with signal to noise ratio up to $13dB$. To increase data rate, 16-OAM and 64-OAM are required if the SNR is sufficient. Therefore, we must make a compromise between the quality of communication and the desired data rate.

V. THEORETICAL BER STUDY

A. Euclidean Distance and Error Probability

In this study, the signal constellation approach is used to develop the error probability formula. Indeed, the error probability depends on the Euclidean distance between signal constellations. Consider two signals s_1 and s_2, separated by the Euclidean distance:

$$d_{12}^2 = \|s_1 - s_2\|^2 \tag{11}$$

The probability of error is given by equation (12) [11] – [14]:

$$P(s_1, s_2) = Q(\sqrt{\frac{d_{12}^2}{2N_0}})$$
$$Q(x) = \frac{1}{2} * erfc(x/\sqrt{2}) \tag{12}$$

B. Modulations associated to IR-UWB

Symbols are represented by the orthogonal basis (f_1, f_2).

1) PPM modulation: For pulse $w(t)$, we can take for example Gegenbauer function of order 1. The two used symbols are $s_1(t) = w(t)$ and $s_2(t) = w(t - \delta)$, this is may be written as:

$$s_1(t) = f_1(t) + f_2(t) \ and \ s_2(t) = f_1(t) - f_2(t) \tag{13}$$

The two symbols are orthogonal:

$$\int s_1(t)s_2(t)dt = 0 \tag{14}$$

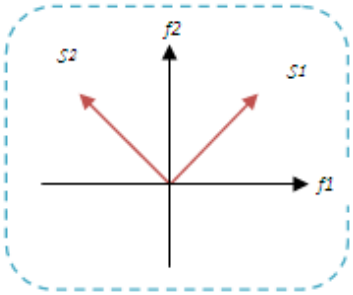

Fig. 7: PPM modulation

The constellation of PPM modulation is illustrated in figure 7. It's an orthogonal PPM. The minimum distance between s_1 and s_2 is: $d_{min} = \sqrt{2} * ||s1||$. The error probability is given by:

$$P_e = Q(\sqrt{\frac{E_p}{N_0}}) \ or \ P_e = \frac{1}{2} * erfc(\sqrt{\frac{\gamma_d}{2}}) \tag{15}$$

E_p : Average energy

2) 4-OAM modulation: In our case, we have 2 bits per symbol: the first bit determines the sign of pulse while the second determines its position.

p_1 and p_2 are the two symbols used for the PPM modulation with:

$$p_1(t) = m(t) \ and \ p_2(t) = m(t - \delta) \tag{16}$$

$m(t)$ is the used waveform and δ the offset characterizing the PPM modulation and equal to the pulse length. The two symbols are orthogonal:

$$\int p_1(t)p_2(t)dt = 0 \tag{17}$$

Knowing that 4-OAM modulation is a combination of PPM modulation (orthogonal symbols) and antipodal modulation (antipodal symbols). Thus, it's a bi-orthogonal modulation.

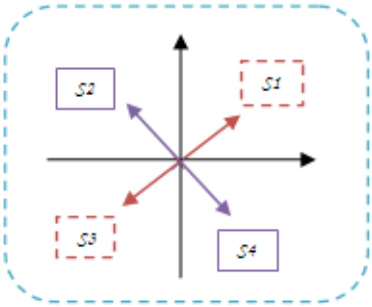

Fig. 8: M-OAM Modulation

The minimum distance between symbols is: $d_{min} = \sqrt{2} * ||s1||$. Error probability is given by:

$$P_{e4-OAM} = \frac{1}{2} * erfc(\sqrt{\frac{E_m}{2N_0}}) \tag{18}$$

With:
E_m: Average energy
N_0: Noise Power Spectral Density

Figure 9 gives a comparison between the results obtained by simulations of BER and analytical calculations of error probability P_e.

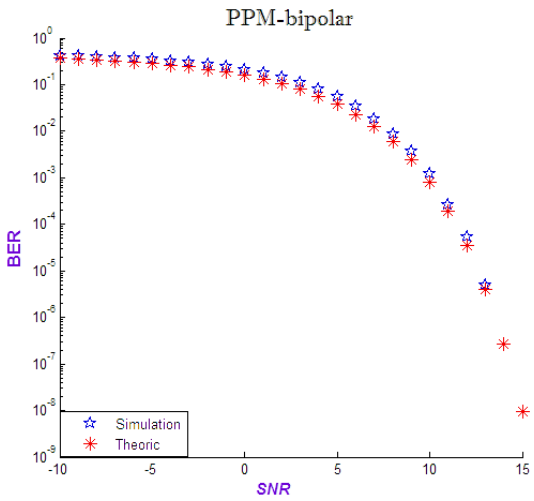

Fig. 9: 4-OAM modulation

We note that simulation results of 4-OAM modulation give the same performance as analytical computation. Consequently, the simulation work of our system is validated by an analytical study.

3) 16-OAM and 64-OAM modulation: The general equation of M-OAM signal is:

$$e(t) = \sum_{k=0}^{N} \sqrt{E_s}/N_p \sum_{p=0}^{N_{p-1}} (2b_{2^{N_p}k+2p} - 1) \; m(t + 2b_{2^{N_p}k+2p+1}\delta + kT) \quad (19)$$

According to figure 4, we have two correlations, each one gives an information on two bits and the decision of each correlation is independent of the other one. Thus, the two correlations are independent. In addition, we have the equiprobable symbols. As a result, the bit error probability is given by:

$$P_{e16-OAM} = \frac{1}{2} * erfc(\sqrt{\frac{E_m}{4N_0}}) \quad (20)$$

The same for 64-OAM modulation: it's a concatenation of three 4-OAM modulations, taking into account the probability of occurrence of each symbol (1/16) and the symbol energy which is six times the bit energy. In the 64-OAM, three independent correlations are considered: the first with G1, the second with G2 and the third with G3. This independence of correlations is due to the orthogonality of Gegenbauer functions. As a result, the bit error probability is given by:

$$P_{e64-OAM} = \frac{1}{2} * erfc(\sqrt{\frac{E_m}{6N_0}}) \quad (21)$$

To evaluate the performance and robustness of this modulation under noise effect, the transmission chain with 4, 16 and 64-OAM modulations is implemented in AWGN channel with coherent receiver. Then, we compared the simulation results with analytical study. Figure 10 illustrates this comparison for three cases of M-OAM modulation.

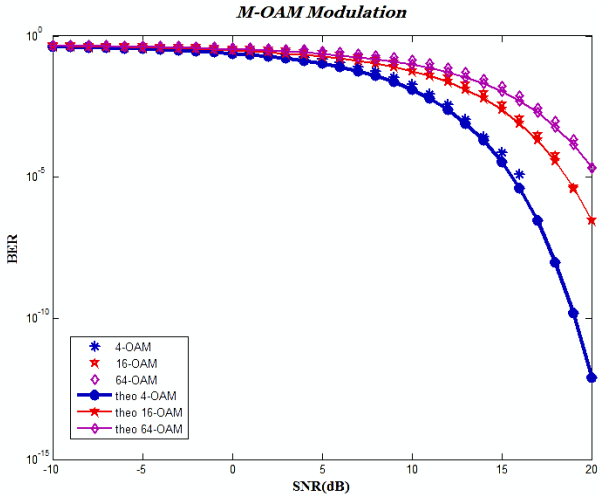

Fig. 10: M-OAM modulation

TABLE VII: Characteristics of different IEEE 802.15.3achannels

Model	CM1 : 0-4m (LOS)	CM2 : 0-4m (NLOS)	CM3: 4-10m (NLOS)	CM1 : > 10 m (NLOS)
Lam	0.0233	0.4	0.0667	0.0667
Lamnbda	2.5	0.5	2.1	2.1
Gam	7.1	5.5	14.00	24
Gamma	4.3	6.7	7.9	12
std_ln_1	$4.8/\sqrt{2}$	$4.8/\sqrt{2}$	$4.8/\sqrt{2}$	$4.8/\sqrt{2}$
std_ln_2	$4.8/\sqrt{2}$	$4.8/\sqrt{2}$	$4.8/\sqrt{2}$	$4.8/\sqrt{2}$
Nlos	0	1	1	1
Std_shdw	3	3	3	3

Figure 10 gives the bit error rate (BER) of M-OAM modulation. We notice that by increasing the number of symbols M, the BER performance of M-OAM modulations deteriorates due to decreasing of Euclidean distance between symbols. In addition, both approaches provide same results. We can therefore conclude that there are no difference between the results of analytical study considered as a reference with those of simulations. This proves the robustness of the proposed modulations.

VI. PERFORMANCE OVER IEEE.802.15.3A CHANNELS ANS S-RAKE RECEIVER

The study of propagation channel effect is an important step in the implementation of any system, especially for those in development step, as is the case of our UWB system. This section studies the IEEE.802.15.3a channels and their implementation in our system with M-OAM modulations.

A. IEEE.802.15.3a standard

IEEE 802.15.3a is based on the formalism of Saleh and Valenzuela (S-V). IEEE 802.15.3a channel presents some specific characteristics: it's a real model and the amplitudes decay follows a law lognormal instead of an exponential decay in S-V model [20]−[22]. Four sets of model parameters are provided for four types of channels. Table VII shows the IEEE.802.15.3a channels characteristics.

B. Simulation results

To examine the performance of our system, transmission chain is simulated. It contains the transmitter using 4-OAM modulations with Gegenbauer waveforms, the 802.15.3a channel with CM1 to CM4 models, and the receiver based on correlation function. Figure 11 exposes the BER versus SNR for each model.

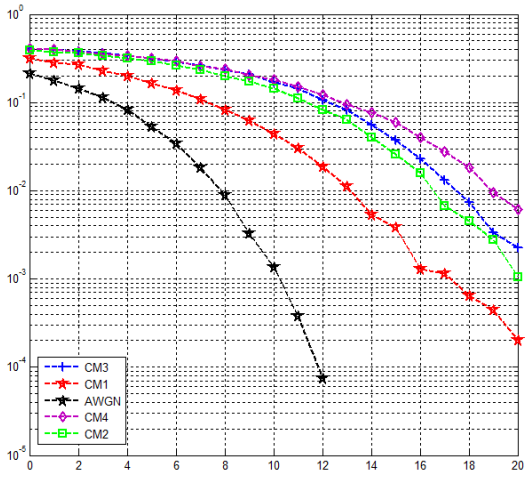

Fig. 11: Comparison between the system performance under AWGN and IEEE 802.15.3a channels

We note that the slope differs between AWGN and CM1-4 channels. Before the introduction of UWB channels, the BER has values less than 10^{-4} for a SNR greater than $10dB$. While with the channel effects, there is a significant signal degradation which increased the value of BER up to 10^{-2} for CM1 for the same value of SNR.

According to table VII and simulation results, we deduce that CM1 offers the best conditions of propagation. However, the other channels give more performance degradation. For that, we focus in the next section on performance improvement solutions.

C. Performance improvements

The transmitted signal undergoes several deformations due to channel effect which produce the phenomenon of inter-symbols interferences (ISI). This phenomenon increases the bit error rate and then degrades the quality of transmission. Several solutions have been proposed in the literature to eliminate ISI interferences. The most used are the equalization techniques, as well as the Rake receiver using multipath constructively. In this section, we will improve the results obtained previously by implementing the Rake receiver. Figure 12 shows the simulation results of our M-OAM system with $S-Rake$ receiver with 5 fingers over UWB channels.

The implementation of S-RAKE receiver leads to significant performance improvements for all models. For an $BER = 2.10^{-3}$, we have an improvement of $3dB$ for $CM1$ and $5dB$ for $CM3$. Thus, the RAKE receiver gives more improvements with $CM3$ model than $CM1$. However, the introduction of Rake receiver with $CM4$ channel does not provide a significant improvement in system performance. This can be explained by the extreme conditions of $CM4$ channel, which is a NLOS environment with a transmitter/receiver distance that exceeds $10m$. To conclude, this section clarifies the contribution of $S-RAKE$ receiver for performance improvement of M-OAM system over IEEE 802.15.3a channels. The next section presents the experimental tests of our M-OAM system in real channel.

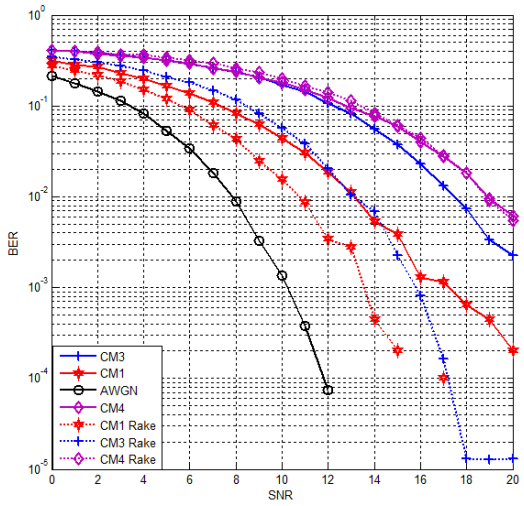

Fig. 12: Contribution of RAKE receiver in M-OAM performance improvement over UWB channels

VII. EXPERIMENTAL TESTS

This part of work is performed in IEMN-DOAE laboratory in indoor environment to take into account of equipment effects and real channel conditions.

A. Manipulation equipments

To validate our proposed M-OAM system, tests are realized using the following general structure (figure 13).

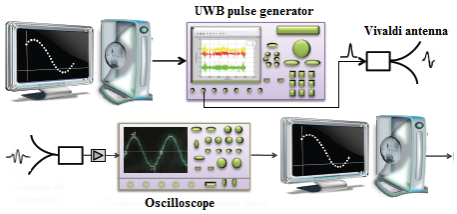

Fig. 13: Manipulation structure

This architecture is composed of a pulse generator provides pulses with a bandwidth which exceeds 3 GHz, two Vivaldi antennas, a preamplifier connected to the receiving antenna, an oscilloscope having a bandwidth of 6 GHz and finally a computer to extract the results of different tests, from the Matlab files provided by the oscilloscope.

In order to find the data sent, the received signal is correlated with the reference signal. By consequence, we detect the pulses peaks and then we recover our data.

B. Experimental results

We chose the 4-OAM modulation with $G1$ waveform. The pulses are generated with amplitude $1V$ peak to peak and

width $550ps$. We use packets of 180 data symbols. Each symbol consists of $111samples$ and the order of $5.5ns$. The transmitter and receiver are on the same axis at a distance of $5m$.

The first step is the construction of references $G1$ that will be used in the correlation with received signal. Thus, the received signal of $G1$ pulse is considered after passage through the two antennas separated by a reasonably low distance.

Figure 14 exposes the shape of reference signal.

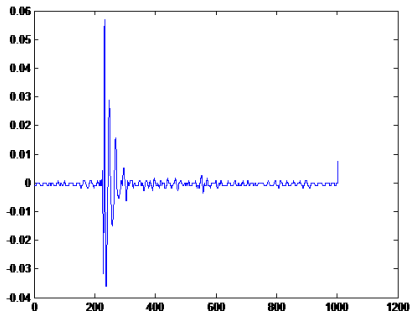

Fig. 14: Reference signal G1

To solve the problem of synchronization between the transmitter/receiver and then find the beginning of sent data, a training sequence is used at the beginning of each packet. Figure 15 presents transmitted (a) and received training sequence (b) based on monocycle pulses modulated with bipolar modulation:

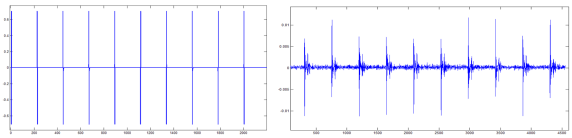

(a) Transmitted TS (b) Received TS

Fig. 15: reference signal

Figure 16 and 17 highlight the transmitted and received signals respectively:

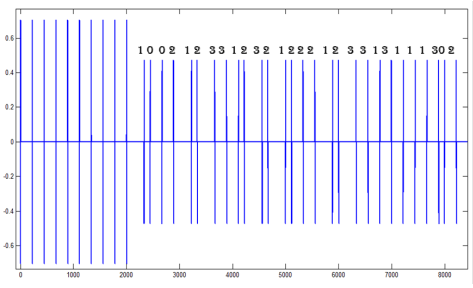

Fig. 16: Transmitted 4-OAM signal

Received signal shown in figure 17 is correlated with training sequence and then the user data is extracted. This last is correlated with reference pulse $G1$ to verify the received data as illustrated in figure 17.

Test results prove that our new system is operational under real conditions of propagation channel for a single transmitter/ receiver synchronously.

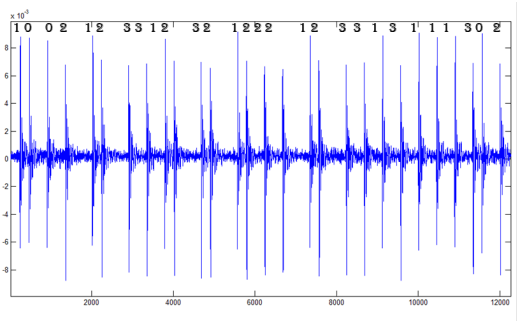

Fig. 17: Received 4-OAM signal

VIII. CONCLUSION

UWB communication systems have appeared for over ten years as a promising solution for new types of wireless networks. It offers flexibility in terms of modulations and receiver architecture. To meet performance and throughput requirements, a new modulation with simple architecture can be adopted.

The main purpose of this paper is to present a new approach of modulations called M-OAM. These modulations are based on replacing the notion of carrier by polynomial order. A comparative study of orthogonal Gegenbauer waveforms is illustrated. To evaluate the performance of proposed system, analytical BER results are compared to the simulation results. It was shown that the proposed system provides a high data rate with good performance and a simplified architecture. However, the multi-path channel effect has a notable impact on the performance of correlation receiver.

Therefore, the contribution of S-RAKE receiver in performance improvement is investigated over UWB channels. Finally, the M-OAM system is validated by many tests in real conditions. Future work will focus on the implementation of this new approach of modulation in FPGA cards.

REFERENCES

[1] D. James Taylor, "Introduction to Ultra Wideband radar system," *CRC Press, Boca Raton*, p.670, 1995.

[2] Agrawal, P. Dharma, and Qing-An Zeng, "Introduction to wireless and mobile systems," *Cengage learning*, 2015.

[3] Official IEEE 802.11 working group project timelines, *IEEE*, 21 septembre 2015.

[4] "IEEE 802.11ac: What Does it Mean for Test?", *LitePoint*, octobre 2013.

[5] M. Ghavami, L.V. Michael, R. Kohno, "Ultra Wide Band Signals and Sytems in Communication engineering," *Ed. Wiley. London*, 247 p., 2007.

[6] B. Parr, B . Cho, K. Wallace, Z. Ding, "A novel ultra-wideband pulse design algorithm," *IEEE Commun. Lett. 7*, 2003, 219-221.

[7] H. Saghir, M. Heddebaut, F. Elbahhar, J.M. Rouvaen, A. Rivenq, "Train-to-wayside wireless communication in tunnel using ultra-wideband and time reversal," *Ed. Elsevier, Transportation Research Part C: Emerging Technologies*, Vol. 17, No. 1, pp. 81-97, 2009.

[8] K. HAMIDOUN, R. ELASSALI, Y. ELHILLALI, A. Rivenq, K. Elbaamrani and F. Boukour "A new multi-user ultra wide band system based on modified Gegenbauer functions and M-OAM modulation for communication of intelligent transportation systems," *Wireless Personal Communications*, vol. 82, no 4, p. 2115-2134, 2015.

[9] F. Elbahhar, A. Rivenq Menhaj, J.M Rouvaen, "Multi-user Ultra Wide Band communication system based on modified Gegenbauer and Hermite functions," *Wireless Personal communications*, Volume 34, Issue 3, Aout 2005.

[10] K. Hamidoun, R. Elassali, Y. Elhillali, K. Elbaamrani, A. Rivenq and F. Elbahhar, "UWB System Based on the M-OAM Modulation in IEEE. 802.15.3a Channel," *In Doctoral Conference on Computing, Electrical and Industrial Systems*, pp. 507-514, Springer, Berlin, Heidelberg, April 2014.

[11] P. Pagani, P. Pajusco, and S. Voinot, "A study of the ultra-wide band indoor channel: Propagation experiment and measurement results," *in Proc. Int. Workshop on Ultra Wideband Systems*, (Oulu, Finland), Juin 2003.
[12] J.G. Proakis, "Digital Communication," *New Work. 4^{th} edition. McGraw-Hill*, 2001.
[13] Eng Gee Lim, Zhao Wang, Chi-Un Lei, Yuanzhe Wang, K.L. Man, "Ultra Wideband Antennas - Past and Present," *IAENG International Journal of Computer Science*, 37:3, pp304-314, 2010.
[14] J.G. Proakis, "Digital Communication," *3^{rd} edition, McGraw-Hill*, 1995.
[15] Bernard Sklar , "Digital Communications Fundamentals and Applications," *2^{nd} Edition*, January 2001.
[16] R. ELASSALI, K. HAMIDOUN, Y. ELHILLALI, A. Revinq, F. Elbahhar, K. Elbaamrani and L. Maatougui, "Performance evaluation of high data rate m-oam uwb physical layer for intelligent transportation systems," *Wireless Personal Communications*, vol. 94, no 4, p. 3265-3283, 2017.
[17] EL ABED A, Fouzia Elbahhar, Yassin Elhillali, Atika Rivenq, Raja Elassali,"UWB Communication System Based on Bipolar PPM with Orthogonal Waveforms," *Wireless Engineering and Technology*, 2012, 3, 181-188, March 1^{st}, 2012.
[18] A.Okassa M'foubat, F. Elbahhar and, C. Tatkeu, "A novel Ultra Wide Band Multi-user receiver for transportation systems communication," *University of Lille North France, IFSTTAR, LEOST*, October 2012.
[19] I. Guvenc and H. Arslan, "On the modulation options for UWB systems," *IEEE Conference on Military Communications (MILCOM)*, vol. 2, pp. 892-897, Boston, USA, Oct. 2003.
[20] D. Cassioli, M. Z. Win, and A. F. Molisch, "The Ultra-Wide Bandwidth Indoor Channel — From Statistical Model to Simulations," *IEEE JSAC*, vol. 20, pp. 1247–57, 2002.
[21] A. F. Molisch, J. R. Foerster, and M. Pendergrass, "Channel models for ultrawideband personal area networks," *IEEE Personal Communications Magazine*, vol. 10, pp. 14–21, Dec. 2003.
[22] J. Keignart and N. Daniele, "Channel sounding and modelling for indoor UWB communications," *in Proc. Int. Workshop on Ultra Wideband Systems*, Oulu, Finland, June 2003.